Dynamic Response of an Elastic Plate Containing Periodic Masses

Andrew J. Hull
Autonomous Systems and Technology Department

WARFARE CENTERS
NEWPORT

Naval Undersea Warfare Center Division
Newport, Rhode Island

PREFACE

This work was performed under Project N00014-04-WX-2-0567, "Simplified Structural Acoustic Model for Active Sonar," principal investigator Andrew J. Hull (Code 8212). The sponsoring activity is the Office of Naval Research, program manager David Drumheller (ONR 333).

The technical reviewer for this report was Benjamin A. Cray (Code 821).

Reviewed and Approved: 31 March 2005

James S. Griffin
Head (*acting*), Autonomous Systems and
Technology Department

REPORT DOCUMENTATION PAGE

Form Approved
OMB No. 0704-0188

1. AGENCY USE ONLY (Leave blank)	2. REPORT DATE 31 March 2005	3. REPORT TYPE AND DATES COVERED

4. TITLE AND SUBTITLE

Dynamic Response of an Elastic Plate Containing Periodic Masses

5. FUNDING NUMBERS

PR A821085

6. AUTHOR(S)

Andrew J. Hull

7. PERFORMING ORGANIZATION NAME(S) AND ADDRESS(ES)

Naval Undersea Warfare Center Division
1176 Howell Street
Newport, RI 02841-1708

8. PERFORMING ORGANIZATION REPORT NUMBER

TR 11,663

9. SPONSORING/MONITORING AGENCY NAME(S) AND ADDRESS(ES)

Office of Naval Research
Ballston Centre Tower One
800 North Quincy Street
Arlington VA 22217-5660

10. SPONSORING/MONITORING AGENCY REPORT NUMBER

11. SUPPLEMENTARY NOTES

12a. DISTRIBUTION/AVAILABILITY STATEMENT

Approved for public release; distribution is unlimited.

12b. DISTRIBUTION CODE

13. ABSTRACT (Maximum 200 words)

This report develops an analytical model that incorporates an infinite number of periodically spaced discrete masses into the equations of elasticity of a two-dimensional solid. Two specific problems are addressed. The first is that of a plate with the masses on the bottom edge, and the second is that of a plate with the masses embedded in the medium. The equations of elasticity are transformed into stress field expressions with the appropriate boundary conditions in the wavenumber-frequency domain. These equations are indexed using an integer shift property to obtain expressions of the higher-order dynamics of the system. Once this is accomplished, all the indexed equations of the system are written together in a single matrix equation. The problem is then solved using a truncated set of terms. The model results are compared to previously available low frequency results for solutions involving the flexural wave in the plate. A numerical example is then solved at high frequency that includes higher-order wave motion, and these results are discussed.

14. SUBJECT TERMS		15. NUMBER OF PAGES
Elasticity Theory	Plate Models	40
Equations of Elasticity	Plate Theory	16. PRICE CODE

17. SECURITY CLASSIFICATION OF REPORT	18. SECURITY CLASSIFICATION OF THIS PAGE	19. SECURITY CLASSIFICATION OF ABSTRACT	20. LIMITATION OF ABSTRACT
Unclassified	Unclassified	Unclassified	SAR

TABLE OF CONTENTS

LIST OF ILLUSTRATIONS

DYNAMIC RESPONSE OF AN ELASTIC PLATE CONTAINING PERIODIC MASSES

1. INTRODUCTION

Plate theory has been researched extensively for many years. Early plate and beam theory[1] modeled displacement in thin plates and beams. These early models contain primarily flexural wave dynamics and are inaccurate at high frequencies and wavenumbers. Rotary inertia and shear effects[2] were added to the flexural wave model to obtain more accurate results at increased frequencies. Fully elastic models[3] were developed to incorporate plate dynamics as the wavelengths of energy that propagate in the plate began to approach and surpass the thickness of the plate. Analysis has also been conducted on the dispersion curves of these systems, particularly in the area of free wave propagation.[4-9] To a lesser extent, the mode shapes of these systems have been studied and documented.[10, 11]

The complexity of plate models has increased over the years by the addition of stiffeners (ribs) or masses. The modeling technique for adding a stiffener to the plate is similar to that for adding a discrete mass to the plate. The problem of a fluid-loaded infinite thin plate with infinite sets of parallel stiffeners excited by a point load has been analyzed in a study that modeled the stiffeners as line forces.[12] This problem was extended to include a moment exerted by the stiffeners and forcing functions of plane wave, line, and point forces.[13, 14] The fluid-loaded infinite plate problem was reformulated for a finite number of equally spaced stiffeners[15] and was further studied for randomly spaced stiffeners.[16] The problem of a fluid-loaded, aperiodic-stiffened infinite plate has also been addressed,[17] as has the analysis of a finite-sized plate containing concentrated masses.[18] In these studies,[12-18] the plate model has been either a thin plate or a thin plate with rotary inertia and shear effects. Finally, the problem was modeled using finite elements to produce numerical solutions.[19]

This report presents an analytical model that incorporates an infinite number of periodically spaced masses into the equations of elasticity that model motion and stress in a two-dimensional solid. The formulation of the problem begins with elasticity theory that models the motion in the solid as a combination of dilatational and shear waves. From this theory, an expression for plate displacement is obtained. The displacements are then inserted into stress relationships that are set equal to the forces acting on the structure by the masses. The problem is then written as a

dynamic system, in matrix form, where the left-hand terms represent the zero-order modes and are equal to an infinite number of right-hand terms that represent the masses acting on the structure plus a term that models the plane wave forcing function. Rewriting this zero-order term by increasing and decreasing the mode index results in an expression for the higher-order modes. The integer shift property is then applied to the right-hand side of all of the terms, resulting in an infinite set of equations that model the wave propagation coefficients of all the modes of the structure. This set of equations is truncated to a finite number of terms, and a solution to the displacement and stress field is calculated. Two different cases are examined: (1) where the masses are on the edge of the plate and (2) where the masses reside within the interior of the plate. The solution is compared to a previously solved problem at low frequency where the wavelength of the plane wave forcing function is large compared to the thickness of the plate. A numerical example of a high-frequency problem is included and discussed.

2. ELASTIC PLATE WITH MASSES ALIGNED
ON THE LOWER SURFACE

The first problem analyzed is that of an elastic plate with discrete (point) masses at the bottom edge, as shown in figure 1. The masses on the bottom of the plate are equally spaced a distance of L (meters) in the x-direction and each has a mass per unit length of M (kg/m). The plate has a thickness of h (meters) and is loaded on the top surface with a forcing function. The model is based on the following assumptions: (1) the forcing function acting on the plate is a plane wave at any definite wavenumber and frequency, (2) the corresponding response of the plate is at definite wavenumber and frequency, (3) motion is normal and tangential to the plate in one direction (two-dimensional system), (4) the plate has infinite spatial extent in the x-direction, (5) the masses have translational degrees of freedom in the x- and z-directions, and (6) the particle motion is linear.
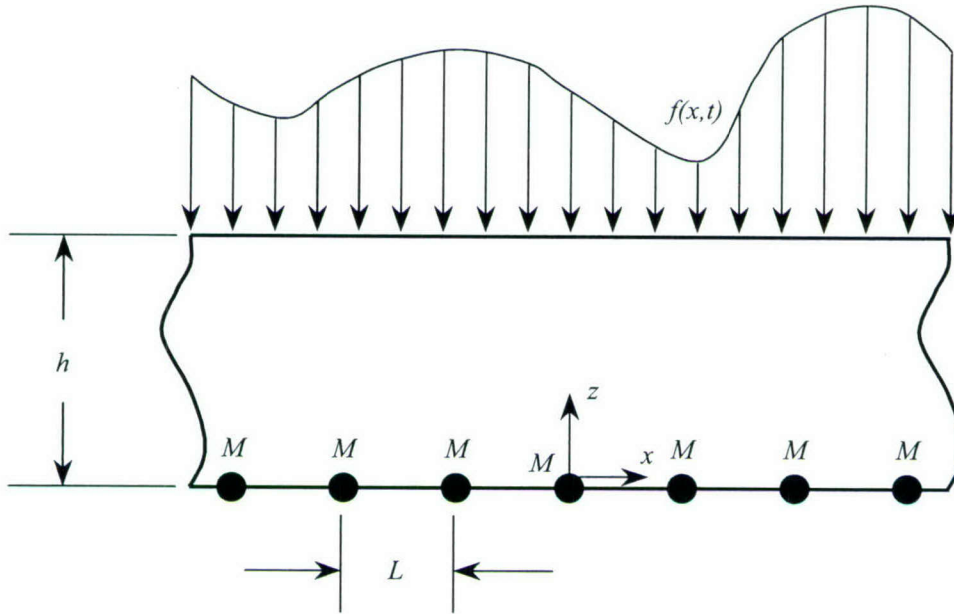
Figure 1. Elastic Plate with Periodic Edge Masses

The motion of the elastic plate is governed by the equation[20]

$$\mu \nabla^2 \mathbf{u} + (\lambda + \mu)\nabla\nabla \bullet \mathbf{u} = \rho \frac{\partial^2 \mathbf{u}}{\partial t^2}, \tag{1}$$

where ρ is the density (kg/m^3), λ and μ are the Lamé constants (N/m^2), t is time (seconds), $\bullet$ denotes a vector dot product, and $\mathbf{u}$ is the two-dimensional Cartesian coordinate displacement vector of the plate. Equation (1) can be expanded and rewritten using four boundary conditions.

The normal stress at the top of the plate ($z = b$) is equal to the opposite of the forcing function and is expressed as

$$\tau_{zz}(x,b,t) = (\lambda + 2\mu)\frac{\partial u_z(x,b,t)}{\partial z} + \lambda\frac{\partial u_x(x,b,t)}{\partial x} = -f(x,t), \tag{2}$$

where $u_z(x,z,t)$ is the displacement in the z-direction (meters), $u_x(x,z,t)$ is the displacement in the x-direction (meters), and $f(x,t)$ is the forcing function exciting the plate expressed in force per unit area (N/m^2). The tangential stress at the top of the plate is zero and is written as

$$\tau_{zx}(x,b,t) = \mu\left[\frac{\partial u_x(x,b,t)}{\partial z} + \frac{\partial u_z(x,b,t)}{\partial x}\right] = 0 . \tag{3}$$

The normal stress at the bottom of the plate ($z = a$) due to the forces induced by the motion of the masses is equal to the summation of the mass multiplied by the acceleration in the z-direction times the spatial delta Dirac function. This expression is

$$\tau_{zz}(x,a,t) = (\lambda + 2\mu)\frac{\partial u_z(x,a,t)}{\partial z} + \lambda\frac{\partial u_x(x,a,t)}{\partial x} = \sum_{n=-\infty}^{n=\infty} M\frac{\partial^2 u_z(x,a,t)}{\partial t^2}\delta(x - nL) . \tag{4}$$

The tangential stress at the bottom of the plate is equal to the summation of the mass multiplied by the acceleration in the x-direction times the spatial delta Dirac function. This equation is written as

$$\tau_{zx}(x,a,t) = \mu\left[\frac{\partial u_x(x,a,t)}{\partial z} + \frac{\partial u_z(x,a,t)}{\partial x}\right] = \sum_{n=-\infty}^{n=\infty} M\frac{\partial^2 u_x(x,a,t)}{\partial t^2}\delta(x - nL) . \tag{5}$$

It is noted that each mass can also be attached to ground with a parallel spring and damper by replacing the mass times vertical acceleration term

$$M\frac{\partial^2 u_z(x,a,t)}{\partial t^2} \tag{6a}$$

with

4

$$M\frac{\partial^2 u_z(x,a,t)}{\partial t^2} + P\frac{\partial u_z(x,a,t)}{\partial t} + Ku_z(x,a,t) \qquad (6b)$$

in equation (4), where P is the viscous damping coefficient per unit length (Ns/m^2), and K is the spring constant per unit length (N/m^2). This system, shown in figure 2, corresponds to a periodically damped and stiffened plate.
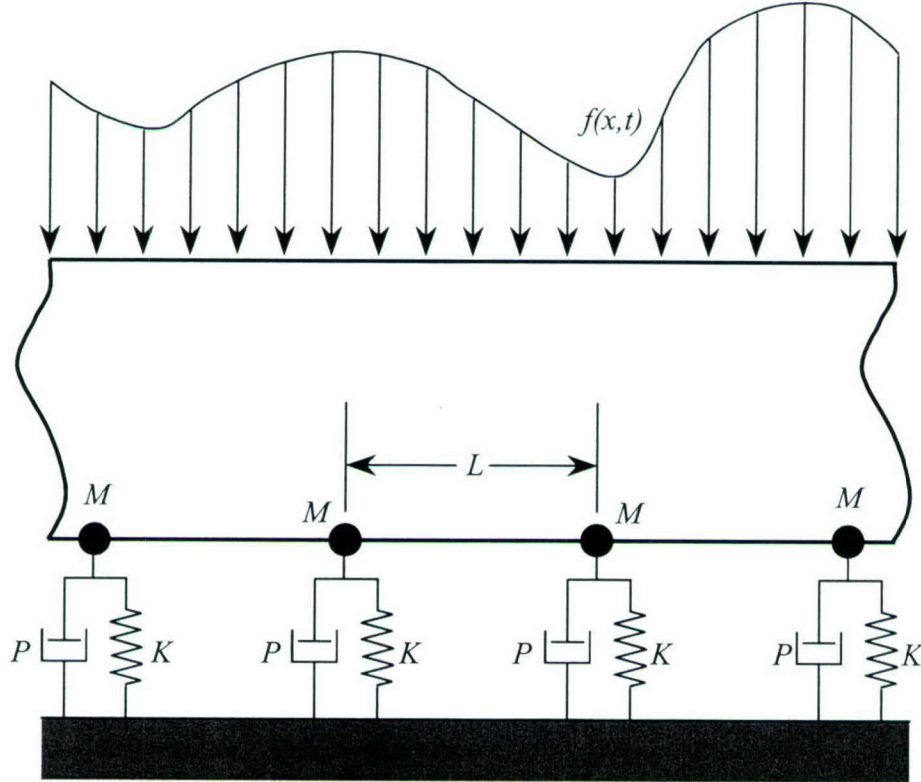
Figure 2. Elastic Plate with Periodic Edge Masses, Dampers, and Springs

Modeling the displacement as a dilatational wave and a shear wave and inserting this term into equation (1) results in the plate displacements

$$u_x(x,z,t) = U_x(k,z,\omega)\exp(ikx)\exp(i\omega t)$$

$$= [A(k,\omega)ik\sin(\alpha z) + B(k,\omega)ik\cos(\alpha z)$$

$$- C(k,\omega)\beta\cos(\beta z) + D(k,\omega)\beta\sin(\beta z)]\exp(ikx)\exp(i\omega t), \qquad (7)$$

and

$$u_z(x,z,t) = U_z(k,z,\omega)\exp(ikx)\exp(i\omega t)$$

$$= [A(k,\omega)\alpha\cos(\alpha z) - B(k,\omega)\alpha\sin(\alpha z)$$

$$+ C(k,\omega)ik\sin(\beta z) + D(k,\omega)ik\cos(\beta z)]\exp(ikx)\exp(i\omega t), \qquad (8)$$

where $A(k,\omega)$, $B(k,\omega)$, $C(k,\omega)$, and $D(k,\omega)$ are complex wave propagation coefficients of the plate (determined by solving the system of equations below); $i = \sqrt{-1}$; ω is the frequency (rad/sec); α is the modified wavenumber (rad/m) associated with the dilatational wave and is expressed as

$$\alpha = \sqrt{k_d^2 - k^2} , \qquad (9)$$

where k_d is the dilatational wavenumber and is equal to ω/c_d, with c_d being the dilatational wavespeed (m/s); β is the modified wavenumber (rad/m) associated with the shear wave and is expressed as

$$\beta = \sqrt{k_s^2 - k^2} , \qquad (10)$$

where k_s is the shear wavenumber (rad/m) equal to ω/c_s, with c_s being the shear wavespeed (m/s); and k is the spatial wavenumber in the x-direction (rad/m). The relationships between the wavespeeds c_d and c_s and the Lamé constants are determined by

$$c_d = \sqrt{\frac{\lambda + 2\mu}{\rho}} , \qquad (11)$$

and

$$c_s = \sqrt{\frac{\mu}{\rho}} . \qquad (12)$$

Equations (2) through (5) are now transferred into the wavenumber-frequency domain using equations (7), (8), and

$$f(x,t) = F\exp(ikx)\exp(i\omega t) , \qquad (13)$$

6

$$\sum_{n=-\infty}^{n=\infty} M \frac{\partial^2 u_x(x,a,t)}{\partial t^2} \delta(x-nL) = -M\omega^2 \left[\sum_{n=-\infty}^{n=\infty} U_x(nL,a,\omega) \exp(-iknL) \right] \exp(i\omega t), \qquad (14)$$

and

$$\sum_{n=-\infty}^{n=\infty} M \frac{\partial^2 u_z(x,a,t)}{\partial t^2} \delta(x-nL) = -M\omega^2 \left[\sum_{n=-\infty}^{n=\infty} U_z(nL,a,\omega) \exp(-iknL) \right] \exp(i\omega t). \qquad (15)$$

Additionally, Poisson's summation formula is applied to the right-hand side of equations (14) and (15), yielding the stresses in the wavenumber-frequency domain as

$$T_{zz}(k,b,\omega) = (\lambda + 2\mu)\frac{\partial U_z(k,b,\omega)}{\partial z} + \lambda \frac{\partial U_x(k,b,\omega)}{\partial x} = -F, \qquad (16)$$

$$T_{zx}(k,b,\omega) = \mu \left[\frac{\partial U_x(k,b,\omega)}{\partial z} + \frac{\partial U_z(k,b,\omega)}{\partial x} \right] = 0, \qquad (17)$$

$$T_{zz}(k,a,\omega) = (\lambda + 2\mu)\frac{\partial U_z(k,a,\omega)}{\partial z} + \lambda \frac{\partial U_x(k,a,\omega)}{\partial x}$$

$$= \frac{-M\omega^2}{L} \sum_{n=-\infty}^{n=\infty} U_z\left(k+\frac{2\pi n}{L}, a, \omega\right), \qquad (18)$$

and

$$T_{zx}(k,a,\omega) = \mu \left[\frac{\partial U_x(k,a,\omega)}{\partial z} + \frac{\partial U_z(k,a,\omega)}{\partial x} \right]$$

$$= \frac{-M\omega^2}{L} \sum_{n=-\infty}^{n=\infty} U_x\left(k+\frac{2\pi n}{L}, a, \omega\right). \qquad (19)$$

Equations (7) and (8) could be inserted into equations (16) through (19); however, the substitution alone would not produce a solution to the problem, because the result would be divergent expressions. Instead, equations (7) and (8) are substituted into equations (16) through (19) and rewritten as

$$[\mathbf{A}^{(0)}(k)]\mathbf{x}^{(0)} = [\mathbf{U}^{(\pm\infty)}(k + \frac{2\pi n}{L})]\mathbf{x}^{(\pm\infty)} + \mathbf{f} \ , \tag{20}$$

with

$$[\mathbf{U}^{(\pm\infty)}(k + \frac{2\pi n}{L})] = \left[\cdots \quad [\mathbf{U}^{(-1)}(k - \frac{2\pi}{L})] \quad [\mathbf{U}^{(0)}(k)] \quad [\mathbf{U}^{(1)}(k + \frac{2\pi}{L})] \quad \cdots \right], \tag{21}$$

where $[\mathbf{A}^{(0)}(k)]$ is a 4 x 4 matrix that models the dynamics of the structure for $n = 0$, $\mathbf{x}^{(0)}$ is the 4 x 1 vector of wave propagation coefficients for $n = 0$, $[\mathbf{U}^{(\pm\infty)}(k + 2\pi n/L)]$ is the 4 x ∞ block-partitioned matrix that represents the periodic mass loading on the structure for $n = -\infty$ to $n = \infty$, $\mathbf{x}^{(\pm\infty)}$ is the ∞ x 1 vector of wave propagation coefficients for $n = -\infty$ to $n = \infty$, and $\mathbf{f}$ is the 4 x 1 vector that models the plane wave excitation. (The entries of the matrixes and vectors in equations (20) and (21) are listed in the appendix.) To facilitate a solution to the problem, the integer shift property of the infinite summation in equation (20) is used. Equation (20) is *m*-indexed and becomes

$$[\mathbf{A}^{(m)}(k + \frac{2\pi m}{L})]\mathbf{x}^{(m)} = [\mathbf{U}^{(\pm\infty)}(k + \frac{2\pi n}{L} + \frac{2\pi m}{L})]\mathbf{x}^{(\pm\infty)} + \mathbf{f}$$

$$= [\mathbf{U}^{(\pm\infty)}(k + \frac{2\pi m}{L})]\mathbf{x}^{(\pm\infty)} + \mathbf{f} . \tag{22}$$

Once the $[\mathbf{A}^{(m)}]$ matrix is integer-indexed and the displacement load matrix indices have been shifted, the system equations can be rewritten using all the *n*-indexed modes as

$$\mathbf{A}\,\mathbf{x}^{(\pm\infty)} = \mathbf{U}\,\mathbf{x}^{(\pm\infty)} + \mathbf{F} \ , \tag{23}$$

where $\mathbf{A}$ is a block-diagonal matrix and is equal to

8

$$
\mathbf{A} = \cdots \begin{bmatrix} \ddots & & \vdots & & & \cdot\cdot \\ & [\mathbf{A}^{(1)}(k+\frac{2\pi}{L})] & & \mathbf{0} & & \mathbf{0} \\ & \mathbf{0} & & [\mathbf{A}^{(0)}(k)] & & \mathbf{0} & \cdots \\ & \mathbf{0} & & \mathbf{0} & & [\mathbf{A}^{(-1)}(k-\frac{2\pi}{L})] \\ \cdot\cdot & & \vdots & & & \ddots \end{bmatrix}, \tag{24}
$$

U is a rank deficient, block-partitioned matrix and is written as

$$
\mathbf{U} = \cdots \begin{bmatrix} \ddots & & \vdots & & \cdot\cdot \\ & [\mathbf{U}^{(-1)}(k-\frac{2\pi}{L})] & [\mathbf{U}^{(0)}(k)] & [\mathbf{U}^{(1)}(k+\frac{2\pi}{L})] \\ & [\mathbf{U}^{(-1)}(k-\frac{2\pi}{L})] & [\mathbf{U}^{(0)}(k)] & [\mathbf{U}^{(1)}(k+\frac{2\pi}{L})] & \cdots \\ & [\mathbf{U}^{(-1)}(k-\frac{2\pi}{L})] & [\mathbf{U}^{(0)}(k)] & [\mathbf{U}^{(1)}(k+\frac{2\pi}{L})] \\ \cdot\cdot & & \vdots & & \ddots \end{bmatrix}, \tag{25}
$$

and **F** is the plane wave load vector

$$
\mathbf{F} = \begin{bmatrix} \cdots & \mathbf{f}^{\mathrm{T}} & \mathbf{f}^{\mathrm{T}} & \mathbf{f}^{\mathrm{T}} & \cdots \end{bmatrix}^{\mathrm{T}}. \tag{26}
$$

The **0** term in equation (24) is a 4 x 4 matrix whose entries are all zeros. Once equation (23) is assembled, the wave-propagation coefficients that reside in the **x** vector can be determined using

$$
\mathbf{x}^{(\pm\infty)} = [\mathbf{A} - \mathbf{U}]^{-1}\mathbf{F}. \tag{27}
$$

When the coefficients are determined, the displacements of the system can be calculated using equations (7) and (8) and the $n = 0$ wave propagation coefficients.

The elastic plate model can be compared and, thus, validated for a thin plate at low frequency using the Bernoulli-Euler differential equation of motion applied to a thin, infinite flat plate containing periodic masses. This model has been previously analyzed[12, 17] using a line load excitation and is reformulated here to correspond to plane wave excitation. This expression is

$$\frac{U_z(k_x,\omega)}{F} = -\left(Dk^4 - \rho h\omega^2\right)^{-1}\left\{1 - \frac{M\omega^2}{L}\sum_{n=-\infty}^{n=\infty}\left[\frac{1}{D\left(k + \frac{2\pi n}{L}\right)^4 - \rho h\omega^2}\right]\right\}^{-1}, \tag{28}$$

where

$$D = \frac{Eh^3}{12(1-\upsilon^2)}. \tag{29}$$

Figure 3 is a plot of the transfer function of displacement in the z-direction divided by input force versus wavenumber at a frequency of 200 Hz. This example was generated with the following system parameters: thickness is 0.01 meter, density is 1200 kg/m³, Lamé constant λ is 2.25×10^8 N/m², and Lamé constant μ is 2.50×10^7 N/m². In figure 3, the dashed line is thin plate theory without the periodic masses (i.e., $M = 0$); the solid line is elastic plate theory with $M = 0.5$ kg/m and $L = 0.1$ meter and corresponds to equations (8) and (27); and the x symbols are thin plate theory with $M = 0.5$ kg/m and $L = 0.1$ meter and corresponds to equation (28). The elastic plate model was calculated using seven modes ($-3 \leq n \leq 3$) that produced a 28- x 28-element, system matrix. The resonance exhibited by the thin plate model is the plate flexural wave. This energy is shifted higher in wavenumber as masses are added to the system. Additionally, the added masses allow energy in the system at characteristic lengths—these effects, called Floquet waves, can be seen at around 20 rad/m and 80 rad/m. The Floquet waves possess stop-bands and pass-bands that correspond to the characteristic lengths of the structure. Notice in figure 3 that the thin and elastic plate models with periodic masses compare closely, but not identically. This is because the elastic plate equations of motion allow the admittance of shear wave effects, rotary inertia, and higher-order wave motion, which are not present in thin plate theory. The transfer function in the x-direction is not shown because the thin plate Bernoulli-Euler equation of motion does not support a degree of freedom in this longitudinal direction.
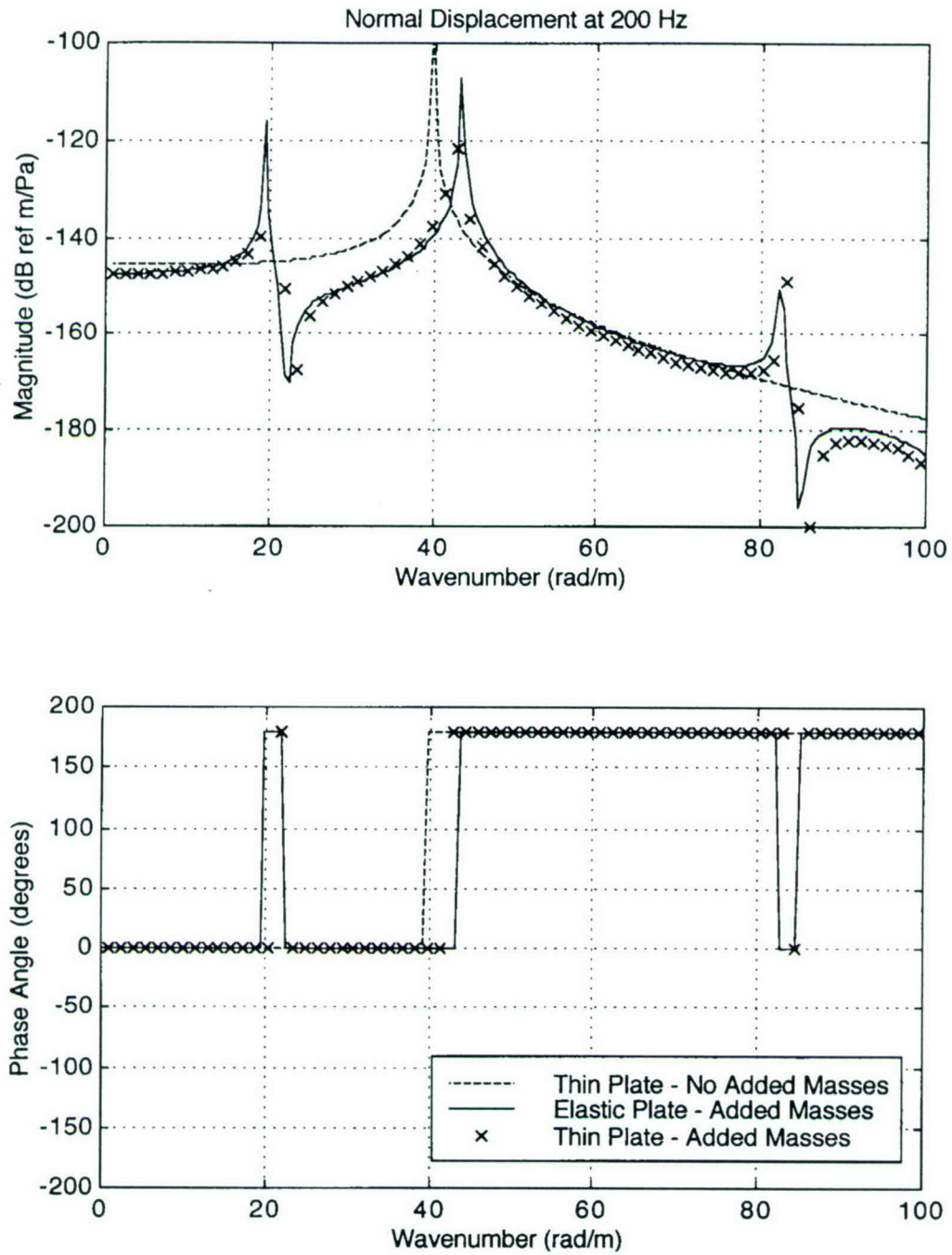
Figure 3. Transfer Function of Displacement Divided by Excitation Force Versus Wavenumber at 200 Hz

Figure 4 is a plot of the elastic plate transfer function calculated using one, three, five, and seven terms compared to thin plate theory for the above example. The wavenumber axis has been expanded to 250 rad/m. This plot illustrates the behavior of the model as more terms are added to the truncated model. Notice that more terms, in general, correspond to dynamics at higher wavenumbers.
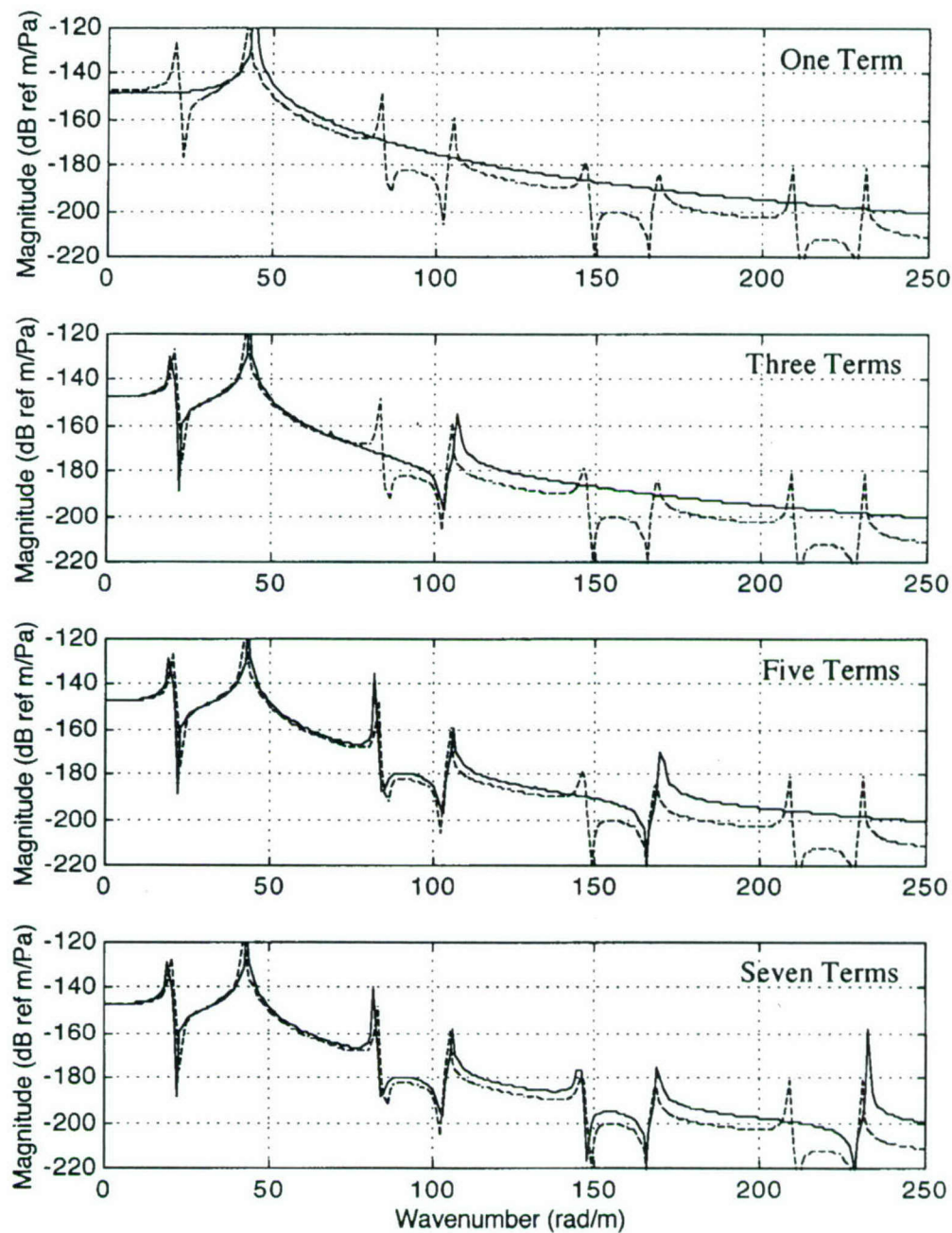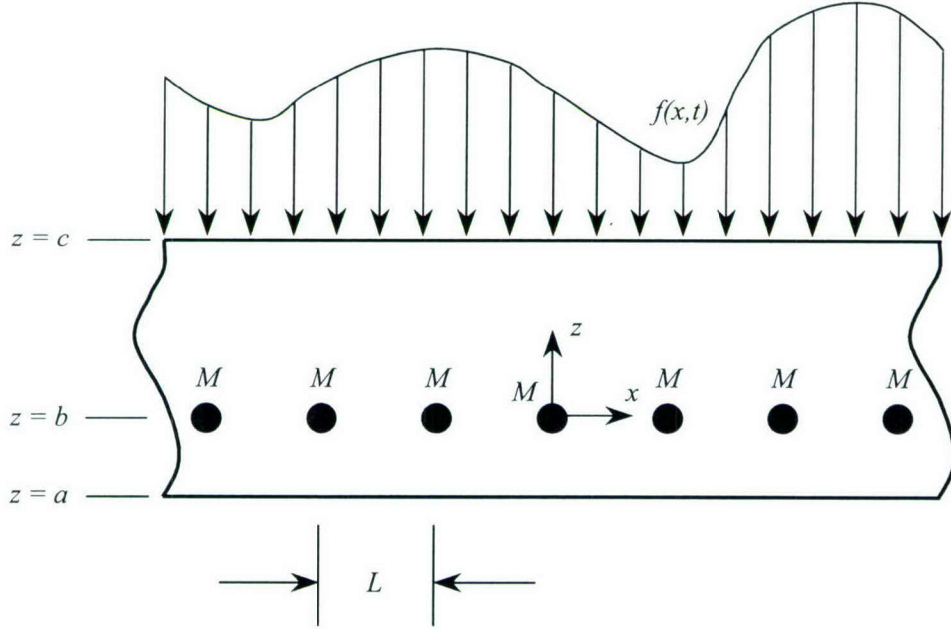

Figure 4. Comparison of the Elastic Plate Transfer Function Calculated Using One, Three, Five, and Seven Terms (Solid Line) and the Thin Plate Theory (Dashed Line)

3. ELASTIC PLATE WITH EMBEDDED INTERIOR MASSES

The elastic plate model can be changed so that the periodic masses are moved from the edge into the interior of the plate, as shown in figure 5.

Figure 5. Elastic Plate with Periodic Interior Masses

The solution to this problem is divided into two parts based on the value of z. The upper region of the plate, location $b \leq z \leq c$, is denoted with a prefix superscript (2), and the lower region of the plate, location $a \leq z \leq b$, is denoted with a prefix superscript (1). The displacement in the x-direction is

$$u_x(x,z,t) = \begin{cases} {}^{(2)}U_x(k,z,\omega)\exp(ikx)\exp(i\omega t) & b \leq z \leq c \\ \\ {}^{(1)}U_x(k,z,\omega)\exp(ikx)\exp(i\omega t) & a \leq z \leq b, \end{cases} \tag{30}$$

where

$$^{(2)}U_x(k,z,\omega) = A(k,\omega)ik\sin(\alpha z) + B(k,\omega)ik\cos(\alpha z)$$

$$- C(k,\omega)\beta\cos(\beta z) + D(k,\omega)\beta\sin(\beta z) \tag{31}$$

and

$$^{(1)}U_x(k,z,\omega) = E(k,\omega)ik\sin(\alpha z) + F(k,\omega)ik\cos(\alpha z)$$

$$- G(k,\omega)\beta\cos(\beta z) + H(k,\omega)\beta\sin(\beta z). \tag{32}$$

The displacement in the z-direction is

$$u_z(x,z,t) = \begin{cases} ^{(2)}U_z(k,z,\omega)\exp(ikx)\exp(i\omega t) & b \le z \le c \\ \\ ^{(1)}U_z(k,z,\omega)\exp(ikx)\exp(i\omega t) & a \le z \le b, \end{cases} \tag{33}$$

where

$$^{(2)}U_z(k,z,\omega) = A(k,\omega)\alpha\cos(\alpha z) - B(k,\omega)\alpha\sin(\alpha z)$$

$$+ C(k,\omega)ik\sin(\beta z) + D(k,\omega)ik\cos(\beta z) \tag{34}$$

and

$$^{(1)}U_z(k,z,\omega) = E(k,\omega)\alpha\cos(\alpha z) - F(k,\omega)\alpha\sin(\alpha z)$$

$$+ G(k,\omega)ik\sin(\beta z) + H(k,\omega)ik\cos(\beta z). \tag{35}$$

There are eight equations of motion that model the system. The first two equations, i.e., (36) and (37), are the normal and tangential stress, respectively, at the top surface of the plate:

$$^{(2)}T_{zz}(k,c,\omega) = -F, \tag{36}$$

and

$$^{(2)}T_{zx}(k,c,\omega) = 0. \tag{37}$$

The next four are the interface equations at the plane on which the masses reside: two (equations (38) and (39)) model the normal and tangential stress balances, respectively, between the upper and lower region of the plate, and the other two (equations (40) and (41)) model the continuity of displacement in the x- and z-directions, respectively. These interface equations are

$$^{(2)}T_{zz}(k,b,\omega) - {}^{(1)}T_{zz}(k,b,\omega) = \frac{-M\omega^2}{L} \sum_{n=-\infty}^{n=\infty} {}^{(1)}U_z(k + \frac{2\pi n}{L}, b, \omega), \tag{38}$$

$$^{(2)}T_{zx}(k,b,\omega) - {}^{(1)}T_{zx}(k,b,\omega) = \frac{-M\omega^2}{L} \sum_{n=-\infty}^{n=\infty} {}^{(1)}U_x(k + \frac{2\pi n}{L}, b, \omega), \tag{39}$$

$$^{(2)}U_z(k,b,\omega) - {}^{(1)}U_z(k,b,\omega) = 0, \tag{40}$$

and

$$^{(2)}U_x(k,b,\omega) - {}^{(1)}U_x(k,b,\omega) = 0. \tag{41}$$

The final two equations of motion are the normal and tangential stress at the bottom surface of the plate:

$$^{(1)}T_{zz}(k,a,\omega) = 0, \tag{42}$$

and

$$^{(1)}T_{zx}(k,a,\omega) = 0. \tag{43}$$

Equations (30) through (35) are now substituted into equations (36) through (43) yielding

$$[\mathbf{B}^{(0)}(k)]\mathbf{y}^{(0)} = [\mathbf{V}^{(\pm\infty)}(k + \frac{2\pi n}{L})]\mathbf{y}^{(\pm\infty)} + \mathbf{g}, \tag{44}$$

where $[\mathbf{B}^{(0)}(k)]$ is an 8 x 8 matrix that models the dynamics of the structure for $n = 0$, $\mathbf{y}^{(0)}$ is the 8 x 1 vector of wave propagation coefficients for $n = 0$, $[\mathbf{V}^{(\pm\infty)}(k + 2\pi n / L)]$ is the 8 x ∞ block-partitioned matrix that represents the periodic mass loading on the structure for $n = -\infty$ to $n = \infty$, $\mathbf{y}^{(\pm\infty)}$ is the ∞ x 1 vector of wave propagation coefficients for $n = -\infty$ to $n = \infty$, and $\mathbf{g}$ is the 8 x 1 vector that models the plane wave excitation. (The matrix and vector entries in equation (44) are listed in the appendix.) The problem solution is identical to that shown in section 2 for the plate with edge masses, although each n-indexed vector has eight entries associated with it instead of the four entries when the masses are on the edge of the plate. Thus, the solution becomes

$$\mathbf{y}^{(\pm\infty)} = [\mathbf{B} - \mathbf{V}]^{-1}\mathbf{G}. \tag{45}$$

The example problem of an elastic plate with discrete masses at the bottom edge was re-analyzed and the displacement results were identical in the z-direction and nearly identical in the x-direction. This indicates that moving the masses into the interior has no effect on the z-displacement and only a slight effect on the x-displacement at this frequency, which is an expected result because this is a low-frequency example where the wavelengths of the forcing function are much larger than the thickness of the plate.

4. NUMERICAL EXAMPLE

A numerical example is now analyzed to show the dynamic response of elastic plates with masses on the edge and in the interior. This example was generated with the following system parameters: thickness is 0.1 meter, density is 1200 kg/m³, Lamé constant λ is 4.5×10^8 N/m², Lamé constant μ is 5.0×10^7 N/m², mass per unit length is 0.5 kg/m, and the mass separation distance is 0.3 meter. Both elastic plate models were calculated using 15 modes ($-7 \leq n \leq 7$) that produced a 60- x 60-element system matrix for the edge mass problem and a 120- x 120-element system matrix for the interior mass problem. For the interior mass problem, the masses were located at the mid-plane of the plate. The displacement values were output at location of $0.25h$ (0.025 meter) from the top of the plate. This problem is constructed so that the wavelengths of the shear and dilatational waves (0.204 and 0.677 meter, respectively) were on the order of the length scales of the plate and mass separation distance.

Figure 6 is a plot of the dispersion curve for the plate with edge masses, which corresponds to free-wave propagation of the system. A frequency range of 0–2000 Hz was chosen so that the first three waves are present in the plot. The three dark, solid lines represent locations in the wavenumber-frequency plane waves that are centered about $k = 0$. These waves are also present in the infinite plate without periodic masses. The other waves (Floquet waves), shown as dashed lines, correspond to waves that share an integer multiple of a characteristic wavenumber. This wavenumber is determined by

$$k_C = \frac{2\pi}{L} \tag{46}$$

and is equal to 20.9 rad/m. These Floquet waves represent energy that is (partially) trapped in the spaces between the periodic masses and is converted into additional free-wave propagation.

Figures 7 and 8 present the transfer function of tangential displacement and normal displacement, respectively, divided by excitation force versus frequency and wavenumber for the plate with edge masses. In both figures, the data are displayed in the decibel scale referenced to meters per Pascal. The free wave that appears in the dispersion curve is clearly evident in both the tangential (figure 7) and normal (figure 8) displacement data. Figures 9 and 10 present the transfer function between tangential displacement and the normal displacement, respectively, and force versus wavenumber at 1000 Hz. Figures 9 and 10 are divided into two plots for clarity; the upper plot is the problem of an elastic plate with edge masses and the lower plot is the elastic

plate with interior masses. The dashed line in all four plots is the elastic plate solution with the absence of masses ($M = 0$).

Upon examination of figures 9 and 10, several features are noted. The energy field has become modally dense as the mass (with its characteristic length) now introduces additional resonances and anti-resonances in the wavenumber space. This result is expected because the model has changed from a continuous, homogeneous infinite structure to a structure that periodically inhibits wave motion by the addition of discrete masses. Additionally, this effect has also been evident in previously developed low-frequency (bending-wave) models. The overall energy levels are approximately the same between the models with masses and the models without masses. This is because higher-frequency models are influenced more by stiffness of the system than by mass. Mass effects are seen more predominately at lower frequencies (see figure 3).
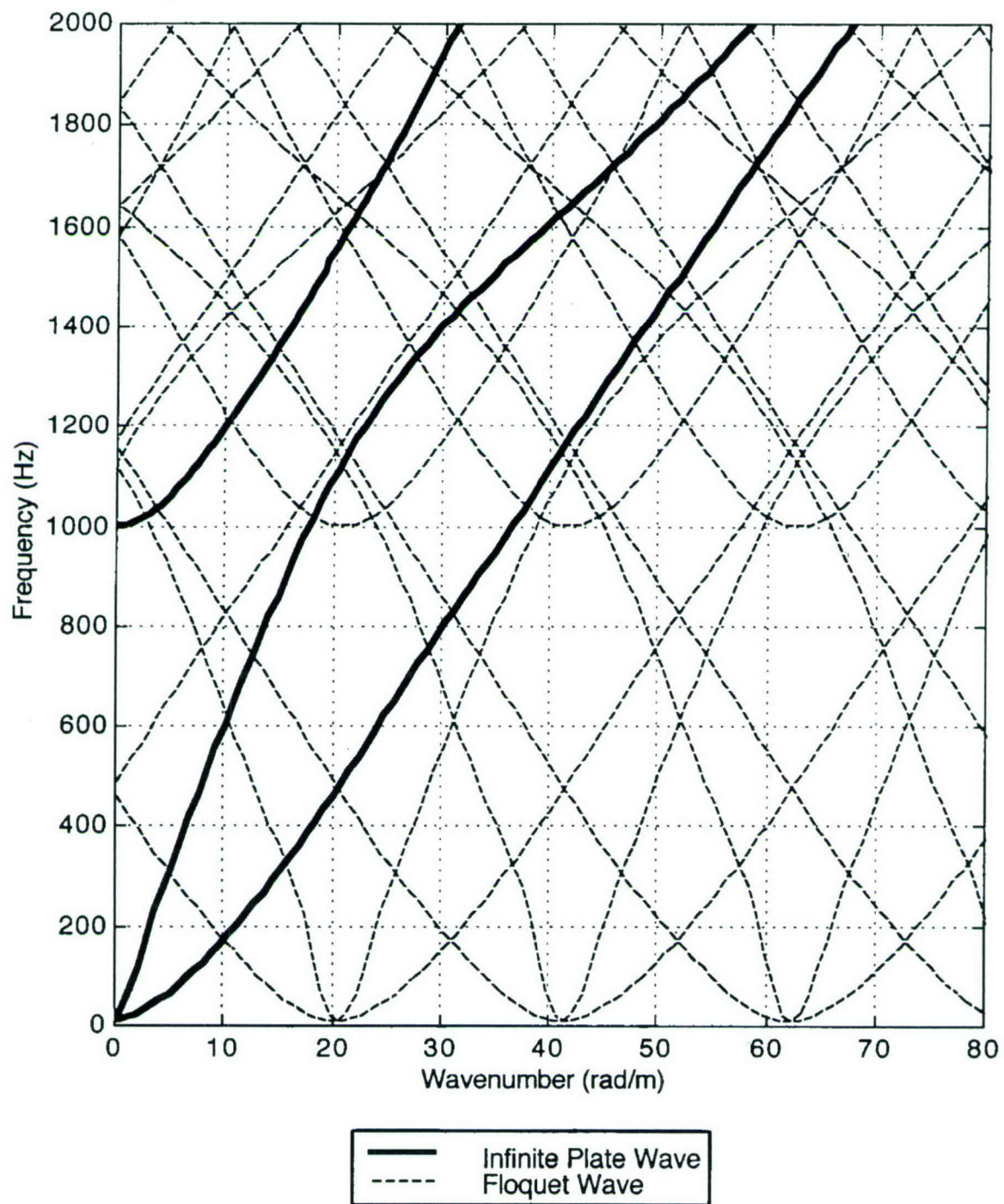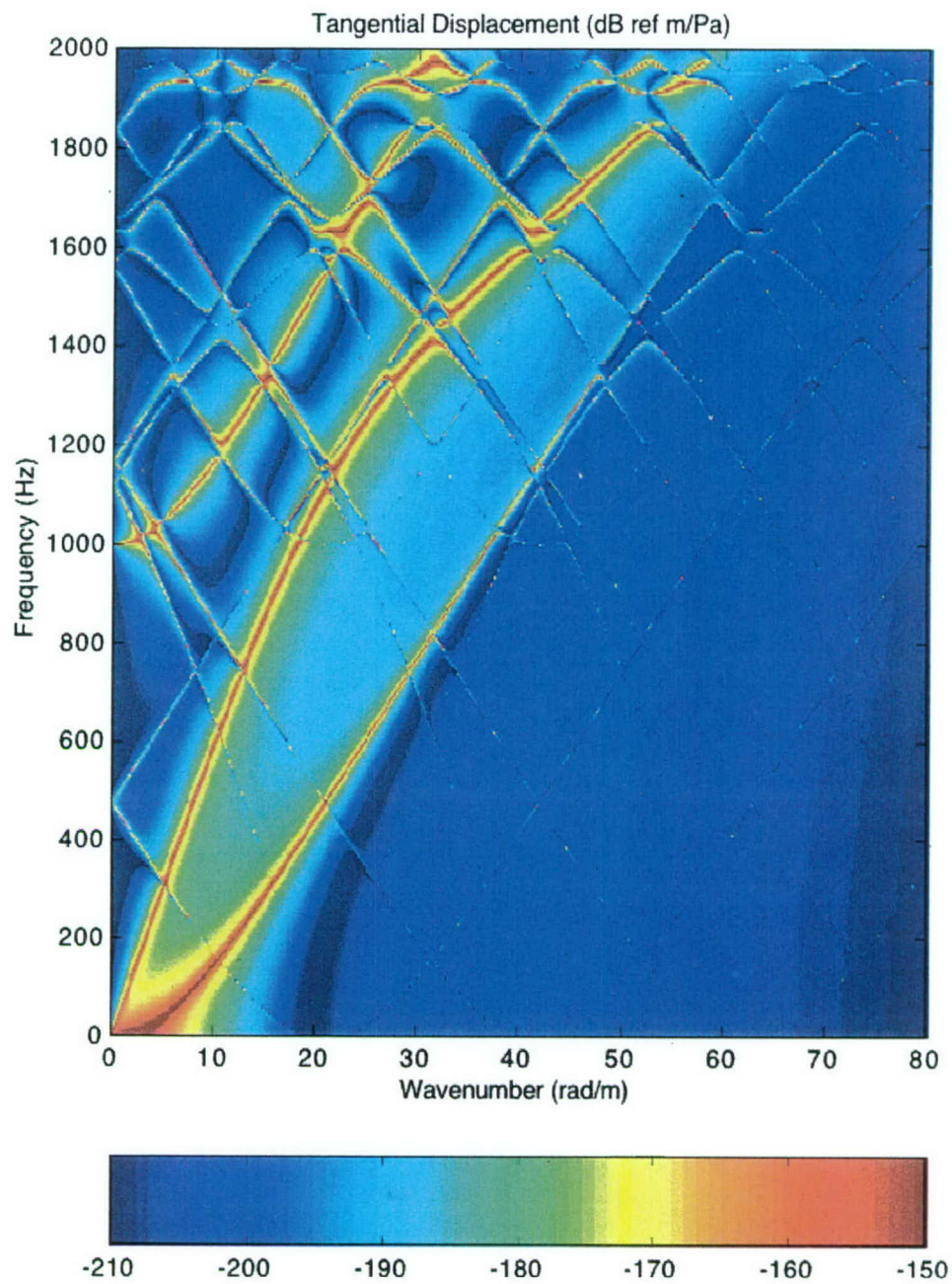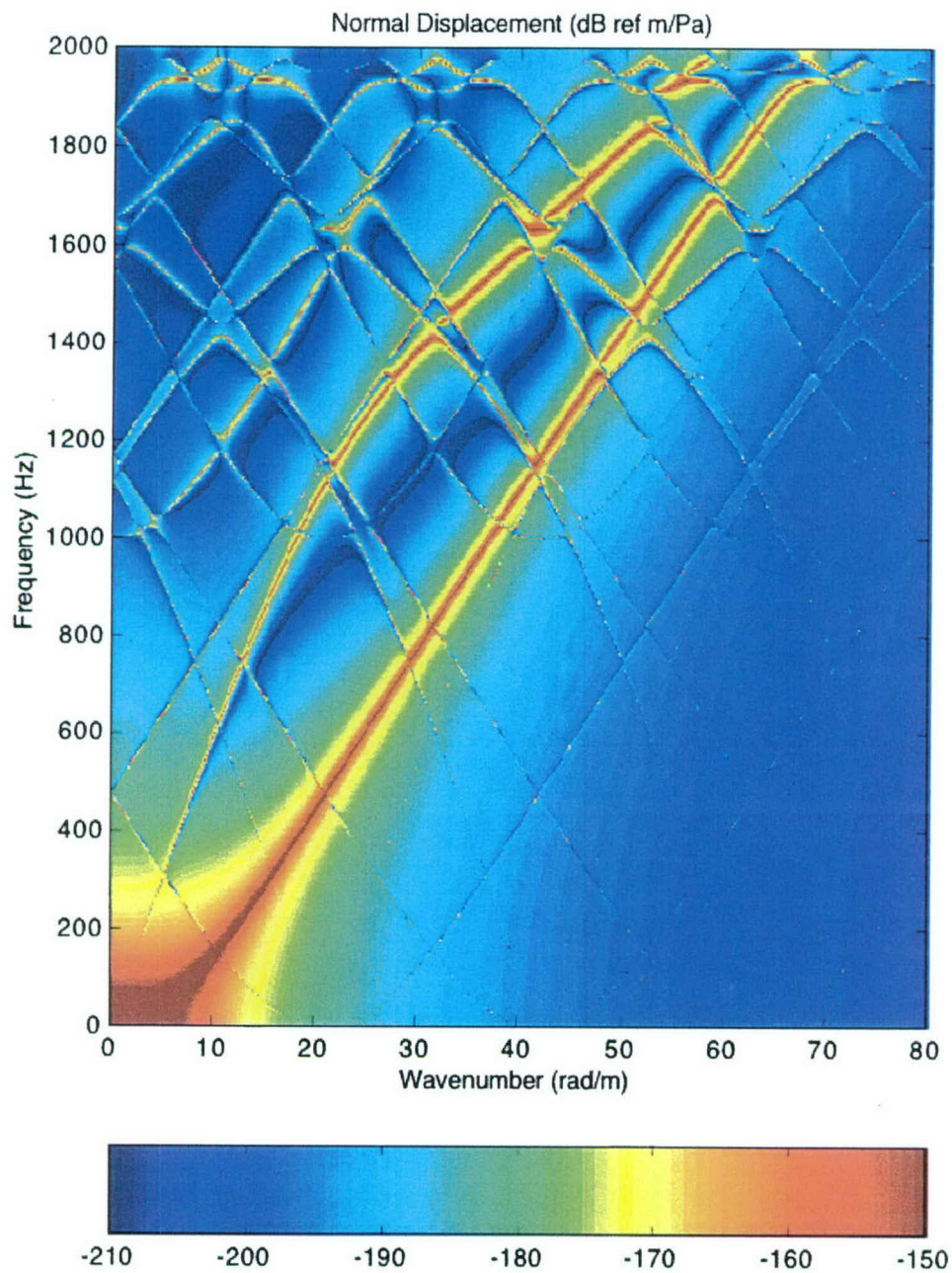
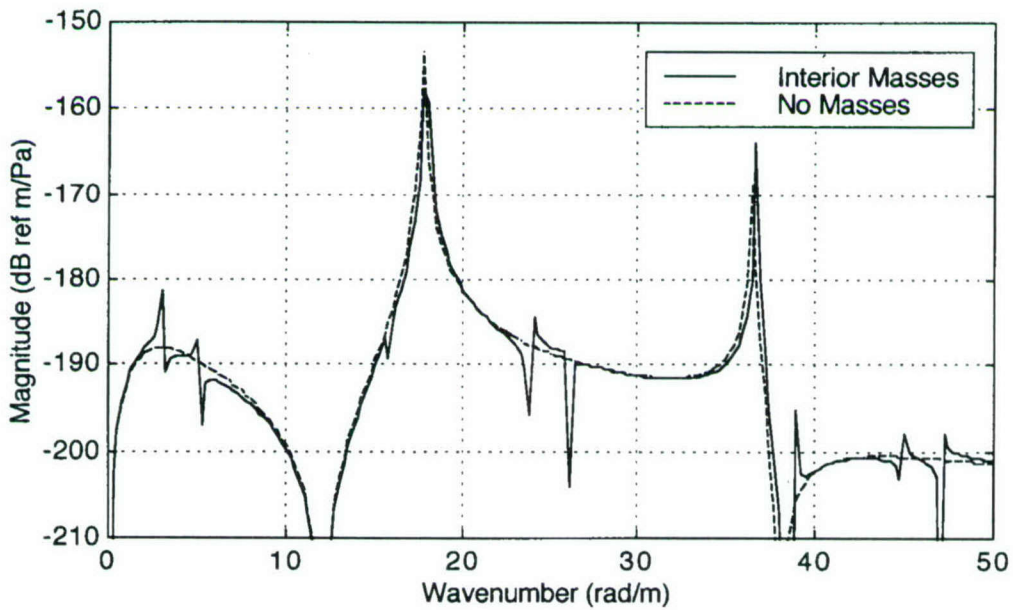**Figure 6. Dispersion Curve of Plate with Edge Masses**

Figure 7. Transfer Function of Tangential Displacement Divided by Excitation Force Versus Frequency and Wavenumber for a Plate with Edge Masses
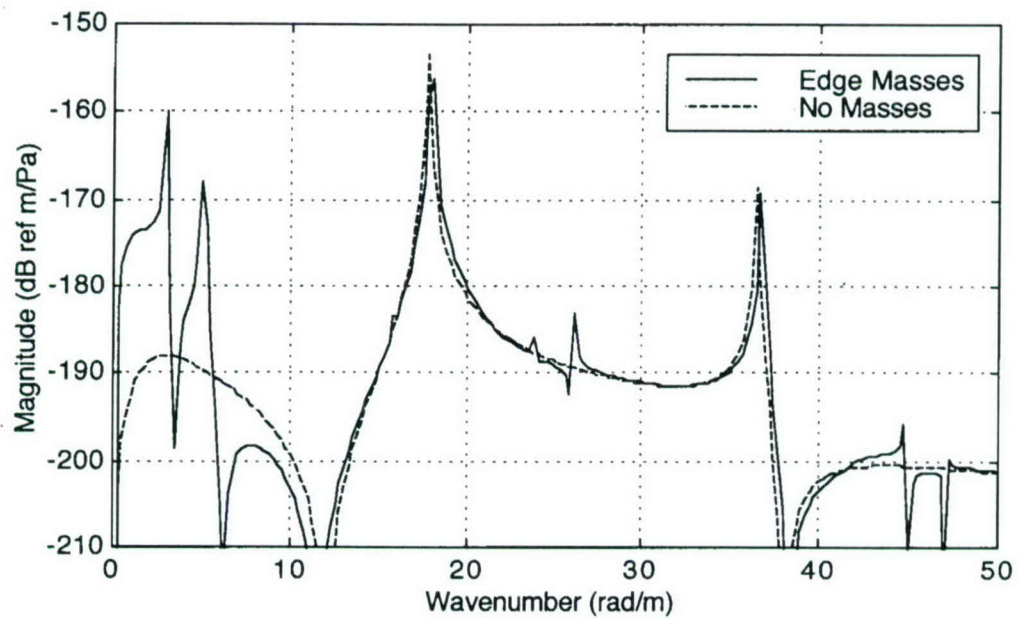
Figure 8. Transfer Function of Normal Displacement Divided by Excitation Force Versus Frequency and Wavenumber for a Plate with Edge Masses

Figure 9. Transfer Function of Tangential Displacement Divided by Excitation Force Versus Wavenumber at 1000 Hz for Edge Masses (Upper Plot) and Interior Masses (Lower Plot)
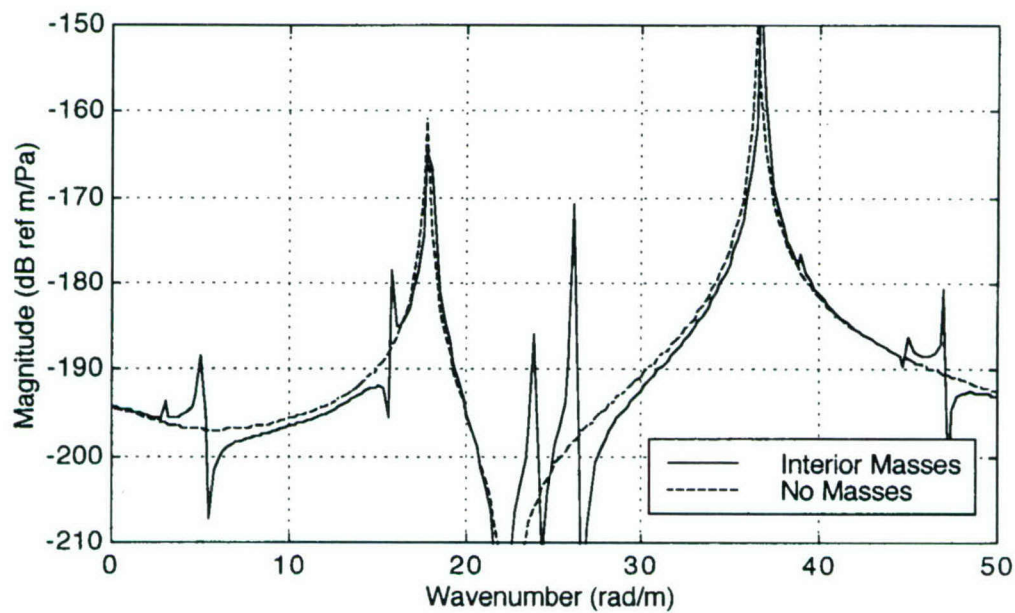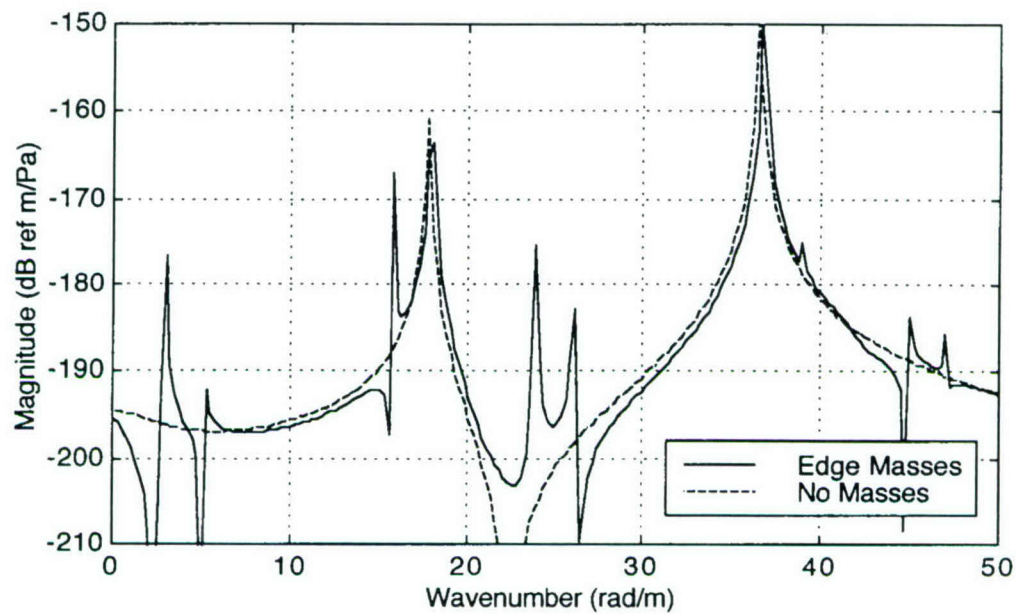
Figure 10. Transfer Function of Normal Displacement Divided by Excitation Force Versus Wavenumber at 1000 Hz for Edge Masses (Upper Plot) and Interior Masses (Lower Plot)

5. CONCLUSIONS

The solution of an elastic plate containing periodic edge and embedded masses has been derived and found to compare favorably with previously developed thin plate models at low frequency. A numerical example of high-frequency dynamics was presented and the details discussed. The dispersion curve and transfer functions of tangential and normal displacements were illustrated. It was shown that the lower- and higher-frequency waves propagate at spatial lengths that correspond to integer multiples of the separation distance of the periodic masses. This characteristic makes the system become modally dense, even at low frequency and low wavenumber.

6. REFERENCES

1. K. F. Graff, *Wave Motion in Elastic Solids*, Dover Publications, New York, 1975.

2. R. D. Mindlin, "Influence of Rotary Inertia and Shear on Flexural Motions of Isotropic Elastic Plates," *Journal of Applied Mechanics*, vol. 18, 1951, pp. 31-38.

3. H. Lamb, "On Waves in an Elastic Plate," *Proceedings of the Royal Society of London Series A*, vol. 93, 1917, pp. 114-120.

4. M. F. M. Osborne and S.D. Hart, 1945, "Transmission, Reflection, and Guiding of an Exponential Pulse by a Steel Plate in Water, I: Theory," *Journal of the Acoustical Society of America*, vol. 17, no. 1, 1945, pp. 1-18.

5. D. G. Crighton, "The Free and Forced Waves on a Fluid-Loaded Elastic Plate," *Journal of Sound and Vibration*, vol. 63, no. 2, 1979, pp. 225-235.

6. A. Freedman, "The Variation, with the Poisson Ratio, of Lamb Modes in a Free Plate, I: General Spectra," *Journal of Sound and Vibration*, vol. 137, no. 2, 1990, pp. 209-230.

7. A. Freedman, "The Variation, with the Poisson Ratio, of Lamb Modes in a Free Plate, II: At Transitions and Coincidence Values," *Journal of Sound and Vibration*, vol. 137, no. 2, 1990, pp. 231-247.

8. J. Dickey, G. Maidanik, and H. Überall, "The Splitting of Dispersion Curves for the Fluid-Loaded Plate," *Journal of the Acoustical Society of America,* vol. 98, no. 4, 1995, pp. 2365-2367.

9. A. Freedman, "Effects of Fluid Loading on Lamb Mode Spectra," *Journal of the Acoustical Society of America,* vol. 99, no. 6, 1996, pp. 3488-3496.

10. A. Freedman, "The Variation, with the Poisson Ratio, of Lamb Modes in a Free Plate, III: Behaviour of Individual Modes," *Journal of Sound and Vibration,* vol. 137, no. 2, 1990, pp. 249-266.

11. A. J. Hull, "Analysis of a Fluid-Loaded Thick Plate," *Journal of Sound and Vibration,* vol. 279, no. 1-2, 2005, pp. 497-507.

12. B. R. Mace, "Sound Radiation from a Plate Reinforced by Two Sets of Parallel Stiffeners," *Journal of Sound and Vibration,* vol. 71, no. 3, 1980, pp. 435-441.

13. B. R. Mace, "Periodically Stiffened Fluid-Loaded Plates, I: Response to Convected Harmonic Pressure and Free Wave Propagation," *Journal of Sound and Vibration,* vol. 73, no. 4, 1980, pp. 473-486.

14. B. R. Mace, "Periodically Stiffened Fluid-Loaded Plates, II: Response to Line and Point Forces," *Journal of Sound and Vibration,* vol. 73, no. 4, 1980, pp. 487-504.

15. G. P. Eatwell and D. Butler, "The Response of a Fluid-Loaded, Beam-Stiffened Plate," *Journal of Sound and Vibration,* vol. 84, no. 3, 1982, pp. 371-388.

16. G. P. Eatwell, "Free-Wave Propagation in an Irregularly Stiffened, Fluid-Loaded Plate," *Journal of Sound and Vibration,* vol. 88, no. 4, 1983, pp. 507-522.

17. B. A. Cray, "Acoustic Radiation From Periodic and Sectionally Aperiodic Rib-Stiffened Plates," *Journal of the Acoustical Society of America,* vol. 95, no. 1, 1994, pp. 256-264.

18. J. W. Nicholson and L.A. Bergman, "Vibration of Thick Plates Carrying Concentrated Masses," *Journal of Sound and Vibration,* vol. 103, no. 3, 1985, pp. 357-369.

19. G. S. Palani, N. R. Iyer, and T. V. S. R. Appa Rao, "An Efficient Finite Element Model for Static and Vibration Analysis of Plates with Arbitrarily Located Eccentric Stiffeners," *Journal of Sound and Vibration,* vol. 166, no. 3, 1993, pp. 409-427.

20. S. P. Timoshenko and J. N. Goodier, *Theory of Elasticity,* McGraw-Hill, New York, 1934.

APPENDIX
MATRIX AND VECTOR ENTRIES

The entries of the matrixes in equations (20) and (21) are listed below. Without loss of generality, the bottom of the plate is defined as $z = a = 0$. For the $[\mathbf{A}^{(n)}(k + 2\pi n/L)]$ matrix, the nonzero entries are

$$a_{11} = (-\alpha_n^2 \lambda - 2\alpha_n^2 \mu - \lambda k_n^2)\sin(\alpha_n h) \ ,$$ (A-1)

$$a_{12} = (-\alpha_n^2 \lambda - 2\alpha_n^2 \mu - \lambda k_n^2)\cos(\alpha_n h) \ ,$$ (A-2)

$$a_{13} = 2i\mu k_n \beta_n \cos(\beta_n h) \ ,$$ (A-3)

$$a_{14} = -2i\mu k_n \beta_n \sin(\beta_n h) \ ,$$ (A-4)

$$a_{21} = 2i\mu k_n \alpha_n \cos(\alpha_n h) \ ,$$ (A-5)

$$a_{22} = -2i\mu k_n \alpha_n \sin(\alpha_n h) \ ,$$ (A-6)

$$a_{23} = \mu(\beta_n^2 - k_n^2)\sin(\beta_n h) \ ,$$ (A-7)

$$a_{24} = \mu(\beta_n^2 - k_n^2)\cos(\beta_n h) \ ,$$ (A-8)

$$a_{32} = -\alpha_n^2 \lambda - 2\alpha_n^2 \mu - \lambda k_n^2 \ ,$$ (A-9)

$$a_{33} = 2i\mu k_n \beta_n \ ,$$ (A-10)

$$a_{41} = 2i\mu k_n \alpha_n \ , \tag{A-11}$$

and

$$a_{44} = \mu(\beta_n^2 - k_n^2) \ , \tag{A-12}$$

where

$$k_n = k + \frac{2\pi n}{L} \ , \tag{A-13}$$

$$\alpha_n = \sqrt{k_d^2 - k_n^2} \ , \tag{A-14}$$

and

$$\beta_n = \sqrt{k_s^2 - k_n^2} \ . \tag{A-15}$$

For the $[\mathbf{U}^{(n)}(k + 2\pi n/L)]$ matrix, the nonzero entries are

$$u_{31} = \frac{-M\omega^2}{L}\alpha_n \ , \tag{A-16}$$

$$u_{34} = \frac{-M\omega^2}{L}ik_n \ , \tag{A-17}$$

$$u_{42} = \frac{-M\omega^2}{L}ik_n \ , \tag{A-18}$$

and

$$u_{43} = \frac{M\omega^2}{L}\beta_n \ . \tag{A-19}$$

The $\mathbf{x}^{(0)}$ vector entries are

$$\mathbf{x}^{(0)} = [A(k,\omega) \quad B(k,\omega) \quad C(k,\omega) \quad D(k,\omega)]^T \equiv \begin{bmatrix} A^{(0)} & B^{(0)} & C^{(0)} & D^{(0)} \end{bmatrix}^T . \quad \text{(A-20)}$$

The $\mathbf{x}^{(\pm\infty)}$ vector entries are

$$\mathbf{x}^{(\pm\infty)} = [\,\ldots \quad A^{(-1)} \quad B^{(-1)} \quad C^{(-1)} \quad D^{(-1)} \quad A^{(0)} \quad B^{(0)}$$
$$C^{(0)} \quad D^{(0)} \quad A^{(1)} \quad B^{(1)} \quad C^{(1)} \quad D^{(1)} \quad \ldots]^T . \quad \text{(A-21)}$$

The $\mathbf{f}$ vector entries are

$$\mathbf{f} = \begin{bmatrix} -F & 0 & 0 & 0 \end{bmatrix}^T . \quad \text{(A-22)}$$

The entries of the matrixes in equation (44) are listed below. Without loss of generality, the location of the masses in the z-direction is defined as $z = b = 0$. For the $[\mathbf{B}^{(n)}(k + 2\pi n / L)]$ matrix, the nonzero entries are

$$b_{11} = (-\alpha_n^2 \lambda - 2\alpha_n^2 \mu - \lambda k_n^2) \sin(\alpha_n c) , \quad \text{(A-23)}$$

$$b_{12} = (-\alpha_n^2 \lambda - 2\alpha_n^2 \mu - \lambda k_n^2) \cos(\alpha_n c) , \quad \text{(A-24)}$$

$$b_{13} = 2i\mu k_n \beta_n \cos(\beta_n c) , \quad \text{(A-25)}$$

$$b_{14} = -2i\mu k_n \beta_n \sin(\beta_n c) , \quad \text{(A-26)}$$

$$b_{21} = 2i\mu k_n \alpha_n \cos(\alpha_n c) , \quad \text{(A-27)}$$

$$b_{22} = -2i\mu k_n \alpha_n \sin(\alpha_n c) , \quad \text{(A-28)}$$

$$b_{23} = \mu(\beta_n^2 - k_n^2)\sin(\beta_n c) \ , \tag{A-29}$$

$$b_{24} = \mu(\beta_n^2 - k_n^2)\cos(\beta_n c) \ , \tag{A-30}$$

$$b_{32} = -\alpha_n^2 \lambda - 2\alpha_n^2 \mu - \lambda k_n^2 \ , \tag{A-31}$$

$$b_{33} = 2i\mu k_n \beta_n \ , \tag{A-32}$$

$$b_{36} = \alpha_n^2 \lambda + 2\alpha_n^2 \mu + \lambda k_n^2 \ , \tag{A-33}$$

$$b_{37} = -2i\mu k_n \beta_n \ , \tag{A-34}$$

$$b_{41} = 2i\mu k_n \alpha_n \ , \tag{A-35}$$

$$b_{44} = \mu(\beta_n^2 - k_n^2) \ , \tag{A-36}$$

$$b_{45} = -2i\mu k_n \alpha_n \ , \tag{A-37}$$

$$b_{48} = -\mu(\beta_n^2 - k_n^2) \ , \tag{A-38}$$

$$b_{51} = \alpha_n \ , \tag{A-39}$$

$$b_{54} = i k_n \ , \tag{A-40}$$

$$b_{55} = -\alpha_n \ , \tag{A-41}$$

$$b_{58} = -i k_n \ , \tag{A-42}$$

$$b_{62} = ik_n \ , \tag{A-43}$$

$$b_{63} = -\beta_n \ , \tag{A-44}$$

$$b_{66} = -ik_n \ , \tag{A-45}$$

$$b_{67} = \beta_n \ , \tag{A-46}$$

$$b_{75} = (-\alpha_n^2 \lambda - 2\alpha_n^2 \mu - \lambda k_n^2) \sin(\alpha_n a) \ , \tag{A-47}$$

$$b_{76} = (-\alpha_n^2 \lambda - 2\alpha_n^2 \mu - \lambda k_n^2) \cos(\alpha_n a) \ , \tag{A-48}$$

$$b_{77} = 2i\mu k_n \beta_n \cos(\beta_n a) \ , \tag{A-49}$$

$$b_{78} = -2i\mu k_n \beta_n \sin(\beta_n a) \ , \tag{A-50}$$

$$b_{85} = 2i\mu k_n \alpha_n \cos(\alpha_n a) \ , \tag{A-51}$$

$$b_{86} = -2i\mu k_n \alpha_n \sin(\alpha_n a) \ , \tag{A-52}$$

$$b_{87} = \mu(\beta_n^2 - k_n^2) \sin(\beta_n a) \ , \tag{A-53}$$

and

$$b_{88} = \mu(\beta_n^2 - k_n^2) \cos(\beta_n a) \ . \tag{A-54}$$

The $[\mathbf{V}^{(n)}(k + 2\pi n / L)]$ matrix can be written as

$$\mathbf{V}^{(n)}(k + \frac{2\pi n}{L}) = \begin{vmatrix} \mathbf{U}^{(n)}(k + \frac{2\pi n}{L}) & \mathbf{0} \\ \\ \mathbf{0} & \mathbf{0} \end{vmatrix},$$ (A-55)

where $[\mathbf{U}^{(n)}(k + 2\pi n / L)]$ is defined in equations (A-16) through (A-19) and $\mathbf{0}$ is a 4 x 4 matrix whose entries are all zero. The $\mathbf{y}^{(0)}$ vector entries are

$$\mathbf{y}^{(0)} = \begin{bmatrix} A(k,\omega) & B(k,\omega) & C(k,\omega) & D(k,\omega) & E(k,\omega) & F(k,\omega) & G(k,\omega) & H(k,\omega) \end{bmatrix}^T$$
$$\equiv \begin{bmatrix} A^{(0)} & B^{(0)} & C^{(0)} & D^{(0)} & E^{(0)} & F^{(0)} & G^{(0)} & H^{(0)} \end{bmatrix}^T.$$ (A-56)

The $\mathbf{y}^{(\pm\infty)}$ vector entries are

$$\mathbf{y}^{(\pm\infty)} = \begin{bmatrix} \cdots & A^{(-1)} & B^{(-1)} & C^{(-1)} & D^{(-1)} & E^{(-1)} & F^{(-1)} & G^{(-1)} & H^{(-1)} \\ \\ & A^{(0)} & B^{(0)} & C^{(0)} & D^{(0)} & E^{(0)} & F^{(0)} & G^{(0)} & H^{(0)} \\ \\ & A^{(1)} & B^{(1)} & C^{(1)} & D^{(1)} & E^{(1)} & F^{(1)} & G^{(1)} & H^{(1)} & \cdots \end{bmatrix}^T.$$ (A-57)

The $\mathbf{g}$ vector entries are

$$\mathbf{g} = \begin{bmatrix} -F & 0 & 0 & 0 & 0 & 0 & 0 & 0 \end{bmatrix}^T.$$ (A-58)

INITIAL DISTRIBUTION LIST

Addressee	No. of Copies
Office of Naval Research (ONR 333: D. Drumheller, K. Ng)	2
Defense Technical Information Center	2
Center for Naval Analyses	1